1

Cosmic rays

1.1 What are cosmic rays?

Cosmic ray particles hit the Earth's atmosphere at the rate of about 1000 per square meter per second. They are ionized nuclei – about 90% protons, 9% alpha particles and the rest heavier nuclei – and they are distinguished by their high energies. Most cosmic rays are relativistic, having energies comparable to or somewhat greater than their masses. A small but very interesting fraction of them have ultra-relativistic energies extending up to 10^{20} eV (about 20 joules), eleven orders of magnitude greater than the equivalent rest mass energy of a proton. The fundamental question of cosmic ray physics is, "Where do they come from?" and, in particular, "How are they accelerated to such high energies?"

The answer to the question of the origin of cosmic rays is not yet fully known. It is clear, however, that nearly all of them come from outside the solar system, but from within the Galaxy. The relatively few particles of solar origin are characterized by temporal association with violent events on the Sun and consequently by a rapid variability. In contrast, the bulk of cosmic rays show an anti-correlation with solar activity, being more effectively excluded from the solar neighborhood during periods when the expanding, magnetized plasma from the Sun – the solar wind – is most intense. The very highest energy cosmic rays have gyroradii in typical galactic magnetic fields that are larger than the size of the Galaxy. These may be of extragalactic origin.

1.2 Objective of this book

The focus of this book is the interface between particle physics and cosmic rays. The two subjects have been closely connected from the beginning, and this remains true today. Until the advent of accelerators, cosmic rays and their interactions were the principal source of new information about elementary particles. The discovery in 1998 of evidence for neutrino oscillations using the neutrino beam produced by

interactions of cosmic rays in the atmosphere is reminiscent of the discoveries of the positron, the muon, the pion and the kaon in the 1930s and 40s. Also, the highest energy cosmic rays can still offer clues about particle physics above accelerator energies, and searches for novel fundamental processes are possible, for example with antiparticles in the cosmic radiation. For the most part, however, cosmic rays are of interest now for the astrophysical information they carry, as reflected by the modern term *particle astrophysics*.

There are important areas in which a knowledge of particle interactions is necessary to understand the astrophysical implications of cosmic ray data. Examples include:

- Production of **secondary cosmic rays** such as antiprotons by primary cosmic rays when they collide with atomic nuclei in the interstellar medium. From the relative amounts of such secondaries we learn about how cosmic rays propagate through the interstellar medium and hence about the nature of the matter and fields that make up the medium.
- Production of **photons, neutrinos** and other particles in collisions of cosmic rays with material near a site of cosmic ray acceleration. Seeing point sources of such particles is a way of identifying specific sources of cosmic ray acceleration and studying how they work. Thus **gamma ray astronomy** and **neutrino astronomy** are closely related to cosmic ray physics, and we will include some discussion of these topics.
- Penetration of **cosmic rays underground** and the detection of muons and neutrinos in large, deep detectors. Such particles can be both signal (for example, neutrinos from the point sources just mentioned) and background (for example, for the search for proton decay or magnetic monopoles). Atmospheric neutrinos are of particular importance because of their use as a beam for the study of neutrino oscillations.
- The relation between **atmospheric cascades** and the incoming cosmic rays that produce them. The highest energy cosmic rays are so rare that they cannot be directly observed with small detectors above the atmosphere, but must be studied indirectly by large air shower arrays exposed for long periods at the surface. Then one has to infer the nature of the primary from its secondary cascade.
- Searches for **exotic particles and new interactions** in the cosmic radiation.

These topics clearly have a great deal in common: the same equations that govern particle cascades in the atmosphere of the Earth also describe particle production by cosmic rays accelerated by a collapsed star which then collide in a surrounding supernova envelope or in the atmosphere of a nearby companion star. The same cross sections that determine the neutrino-induced signal in an underground detector also determine how much energy is absorbed by a companion star due to

interactions of neutrinos produced by cosmic rays accelerated in the system. The purpose of the book is to describe particle interactions in natural environments in a common framework, to describe the detectors and their results, and to discuss the conclusions that can be made about the primary cosmic radiation. The book also includes a summary of cosmic ray origin – propagation, acceleration and sources.

1.3 Types of cosmic ray experiment

The principal data about the cosmic rays themselves, from which one can hope to learn about their origin, are the relative abundances of the different nuclei (composition), the distribution in energy (energy spectrum) of each component and the distribution of arrival directions. Comparison with the chemical composition of various astrophysical objects, such as the Sun, the interstellar medium, supernovae or neutron stars, can give clues about the site at which cosmic rays are injected into the acceleration process. The energy spectra may be characteristic of certain acceleration mechanisms.

Figure 1.1 gives a global view of the total cosmic ray energy spectrum. The fluxes cover an enormous range of energy, from less than a GeV to more than 10^{20} eV: some twelve orders of magnitude. In addition, the flux falls rapidly with energy, so it is necessary to plot the intensity on a log–log scale. Also, it is customary to multiply the differential intensity by a power of energy. Here we plot $E\mathrm{d}N/\mathrm{d}E = \mathrm{d}N/\mathrm{d}\ln E$. Since energy measurements generally have a precision δE, which is proportional to energy, E, this is a natural way to show the event rates that would be expected in detectors that cover different ranges of energy. Often one multiplies the flux by a higher power of energy. For example, $E \times \mathrm{d}N/\mathrm{d}\ln E$ is analogous to the spectral energy density, $\nu F(\nu)$, in multiwavelength astronomy, which shows the energy content per logarithmic interval of energy and thus reflects the physics of the source. Still higher multiplicative powers ($E^{2.5}$, E^3) are sometimes used simply to flatten a steeply falling spectrum to look for structure.

A moment's thought about the range of rates in Figure 1.1 will convince you that several quite different kinds of detectors are necessary to study cosmic rays over this whole energy range. In the interval around 100 GeV, for example, the cosmic ray flux is approximately two particles per square meter per steradian per second. This means that magnetic spectrometers with acceptance of order 0.1 $\mathrm{m}^{-2}\mathrm{sr}^{-1}$ can collect a few thousand events in a day, which is sufficient to measure the spectra of protons and helium up to this energy but not much higher.

A detector system that includes a magnetic spectrometer to bend charged particles can make the most precise measurement of the particle momentum. The left panel of Figure 1.2 shows how the Alpha Magnetic Spectrometer (AMS) identifies an electron and measures its momentum from a precise measurement of bending in

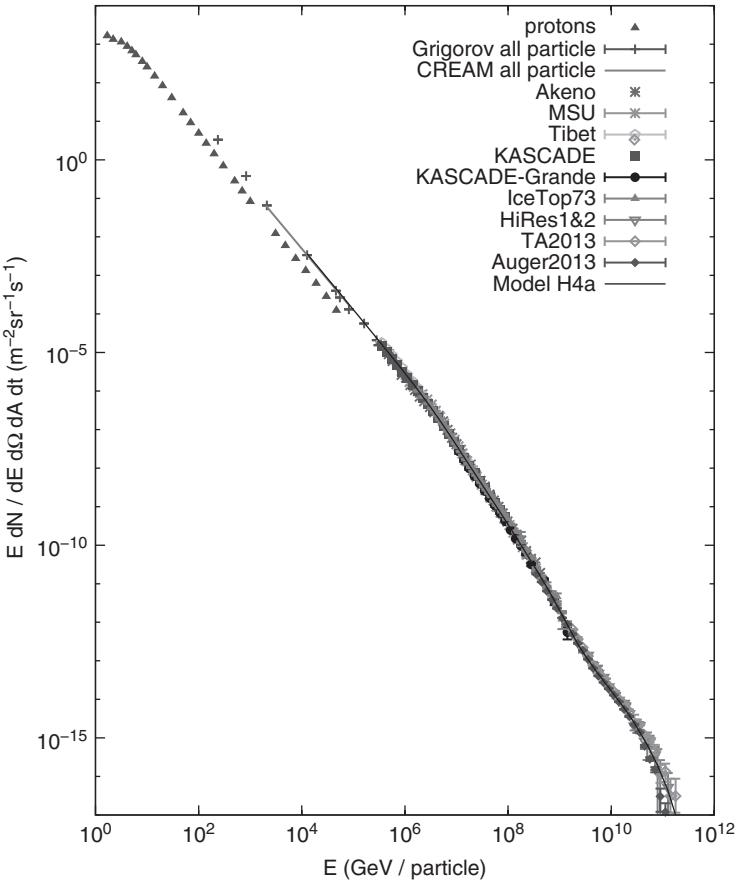

Figure 1.1 Global view of the cosmic ray energy spectrum. The triangles from 1 GeV to 10 TeV give the measured flux of protons. All other data and the model line represent the spectrum of the sum of all nuclei as a function of total energy per nucleus. See Appendix A.2 for references.

the tracking planes inside the magnet. The transition radiation detector (TRD) at the top identifies the particle as an electron and the time of flight (TOF) counters measure the velocity and show that the particle is downward. The TOF scintillators also measure the charge of the particle using the Z^2 dependence of the ionization. The ring imaging Cherenkov (RICH) detector independently determines charge and velocity. Finally, the electron generates a shower in the electromagnetic calorimeter (ECAL) at the bottom confirming its identity and providing an independent measurement of its energy. The maximum energy achievable with a spectrometer is limited by its tracking resolution (which determines the maximum detectable radius of curvature) and by the size of the fiducial region of the magnetic field,

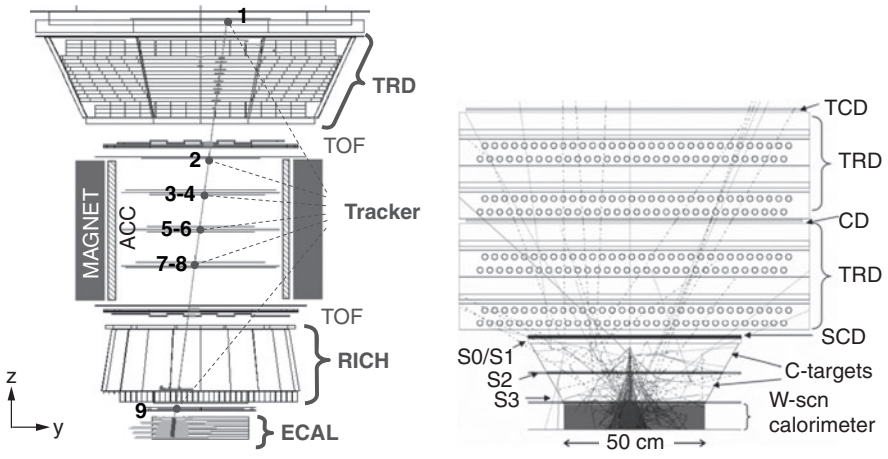

Figure 1.2 Left: Schematic of the AMS02 spectrometer on the International Space Station showing reconstruction of a TeV electron [1]; Right: Schematic of the CREAM calorimeter showing a simulated proton shower [2].

which determines the acceptance of the spectrometer in units of area times solid angle. AMS02 has measured the spectra of protons and helium to somewhat above 1 TeV/nucleon and the spectra of electrons and positrons to several hundred GeV.

One way to go to higher energy while still having a direct identification of the primary particle before it interacts in the atmosphere is to use a calorimeter detector system without a magnetic spectrometer, thus allowing a larger geometrical acceptance. The measurement of the energy is less precise because of fluctuations from event to event in how the cascades develop in the calorimeter coupled with the fact that some of the shower particles punch through the bottom. The right panel of Figure 1.2 shows a simulated proton event in CREAM [2], a calorimeter detector that has been carried on several circumpolar balloon flights in Antarctica, providing measurements of protons, helium and heavier nuclei above a TeV up to more than 100 TeV per particle. The proton data in Figure 1.1 up to a TeV are from AMS02. The higher energy measurements of protons shown are from CREAM.

To study cosmic rays with higher energies requires detectors with larger areas exposed for longer periods of time. At present the only way to overcome the problem of low flux at high energy is to build a detector on the surface of the Earth. Such detectors, called "air shower arrays," can have areas measured in hundreds or even thousands of square kilometers and exposure times of years. Such ground-based detectors cannot detect the primary cosmic rays directly, however. Instead they detect only the remnants of the atmospheric cascade of particles initiated by the incident particle and can therefore give only limited, indirect information about the nature of the primaries themselves. Despite the obvious difficulty of the subject,

the ultra-high energies involved continue to stimulate interest in it. This is clearly an area where a knowledge of particle physics is essential in order to interpret the cascades and infer something about the primaries. We will return to this subject in Chapters 16 and 17 of the book. For now, however, we focus on the bulk of the cosmic rays at lower energies.

1.4 Composition of cosmic rays

Figure 1.3 compares the relative abundances of cosmic rays with abundances of elements in the solar system. Both solar system and cosmic ray abundances show the odd–even effect, with the more tightly bound, even Z nuclei being more abundant. There are, however, two striking differences between the two compositions.

First, nuclei with $Z > 1$ are much more abundant relative to protons in the cosmic rays than they are in solar system material. This is not really understood, but it could have something to do with the fact that hydrogen is relatively hard to ionize for injection into the acceleration process, or it could reflect a genuine difference in composition at the source.

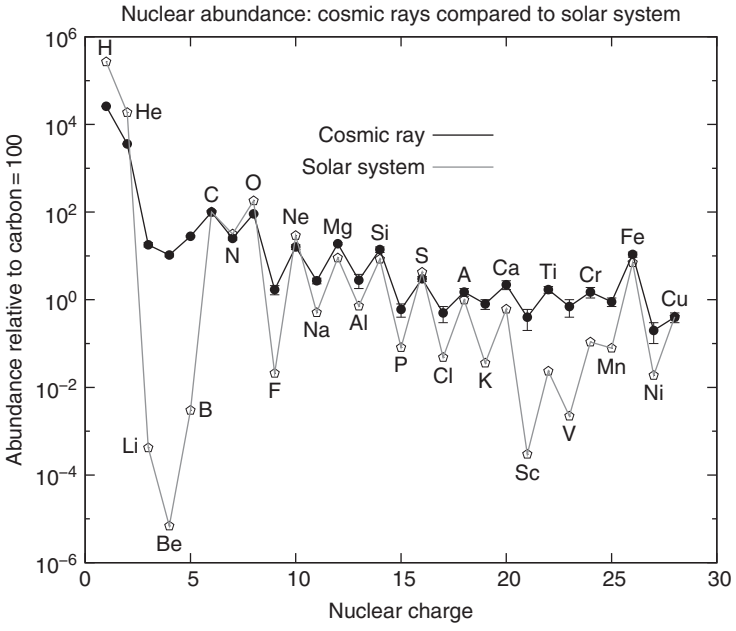

Figure 1.3 The cosmic ray elemental abundances measured on Earth (filled symbols connected by solid lines) compared to the solar system abundances (open symbols), all relative to carbon = 100. This figure is made from Table 9.1 of Ref. [3], which lists both the solar system abundances and the cosmic ray abundances in the GeV range.

The second difference *is* well understood and is an important tool for understanding propagation and confinement of cosmic rays in the galaxy. The two groups of elements Li, Be, B and Sc, Ti, V, Cr, Mn are many orders of magnitude more abundant in the cosmic radiation than in solar system material. These elements are essentially absent as end-products of stellar nucleosynthesis. They are nevertheless present in the cosmic radiation as spallation products of higher mass elements, in particular of carbon and oxygen and of iron, respectively. They are produced by collisions of cosmic rays with the interstellar medium (ISM). From a knowledge of the cross sections for spallation, one can learn something about the amount of matter traversed by cosmic rays between production and observation. (Note the implication that secondaries such as photons, neutrinos and antiprotons should also be produced at a certain rate as cosmic rays propagate through the ISM. We shall return to this subject in Chapter 11.) For the bulk of the cosmic rays the mean amount of matter traversed is of order $X = 5\,\mathrm{g/cm^2}$. The density ρ_N in the disk of the galaxy is of order one proton per $\mathrm{cm^3}$, so this thickness of material corresponds to a distance of

$$\ell = X/(m_p \rho_N) = 3 \cdot 10^{24}\,\mathrm{cm} \approx 1000\,\mathrm{kpc}. \tag{1.1}$$

Since the cosmic rays may spend some time in the more diffuse galactic halo, this is a lower limit to the distance traveled. In any case, $\ell \gg d \approx 0.1$ kpc, the half-thickness of the disk of the galaxy. This implies that cosmic ray confinement is a diffusive process in which the particles rattle around for a long time before escaping into intergalactic space.

1.5 Energy spectra

The spectra for several elements of the cosmic rays are shown in Figure 1.4. The proportions of the major components are relatively constant with energy (see Table 1.1). Note, however, that the boron spectrum is steeper than the spectra of its parent oxygen and carbon nuclei; i.e. the secondary to primary ratio decreases as energy increases. This tells us that the higher energy cosmic rays diffuse out of the galaxy faster.

Cosmic ray composition relative to protons in the 10–1000 GeV range is shown in Table 1.1. The normalization is at 11.5 GeV total energy per nucleon, where the differential flux of protons is $17.6\,\mathrm{m^{-2}s^{-1}sr^{-1}GeV^{-1}}$. The table shows the fraction of nuclei relative to protons in four different ways. Fluxes are normally quoted as in column (1): particles per GeV per nucleon. If we define the fractions in column (1) as F_A (e.g. $F_4 = 0.048$ for helium nuclei), then the fractions in the other columns are related to those in column (1) by $2^\gamma\, F_A$ for column (2); $A\, F_A$ for column (3) and $A^\gamma\, F_A$ for column (4). These relations hold for a power law spectrum with

Table 1.1 *Fraction of nuclei relative to protons*

		(1)	(2)	(3)	(4)
Z (nuclei)	$\langle A \rangle$	particles $> E/A$	particles $> R$	nucleons $> E/A$	particles $> E$/nucleus
1 (p)	1	1	1	1	1
2 (α)	4	0.048	0.157	0.193	0.51
3–5 (Li,Be,B)	9	0.00074	0.00024	0.00087	0.03
6–8 (C,N,O)	14	0.0041	0.0133	0.0570	0.36
9,10 (F,Ne)	20	0.00056	0.0018	0.0111	0.09
11,12 (Na,Mg)	23	0.00041	0.0013	0.0094	0.09
12,13 (Al,Si)	27	0.00035	0.0011	0.0096	0.10
15,16 (P,S)	31	0.00006	0.00018	0.0017	0.02
17,18 (Cl,Ar)	40	0.00002	0.00006	0.0007	0.01
19,20 (K,Ca)	40	0.00004	0.00012	0.0015	0.02
21–25 (Sc-Mn)	48	0.00009	0.00030	0.0044	0.07
26–28 (Fe-Ni)	56	0.00022	0.00072	0.0124	0.21

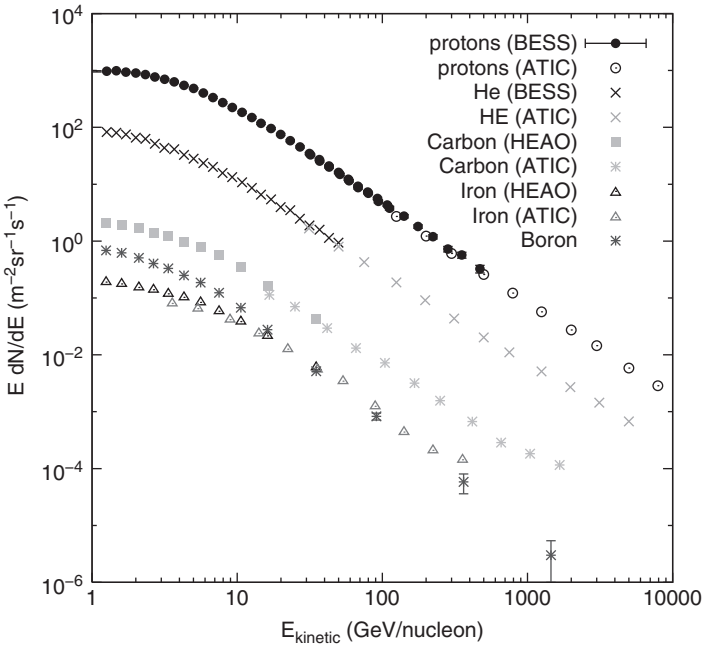

Figure 1.4 Energy spectra of several components of the cosmic rays. For energies less than 10 GeV/nucleon the flux varies significantly during the solar cycle, an effect called "solar modulation."

$N_A(>E) \propto E^{-\gamma}$. In this energy range the integral spectral index $\gamma \approx 1.7$. Note that these relations are for *integral* fluxes, i.e. for relative numbers of each species above the given threshold. Note also that $N(>E) = \frac{1}{\gamma} \times \frac{dN}{d\ln(E)}$ for a power-law spectrum with index $-\gamma$.

Each of the columns is relevant for certain situations. Column (1) (nuclei per energy per nucleon) is appropriate for propagation calculations because energy per nucleon remains essentially unchanged in spallation processes. Column (2) (rigidity, $R(\mathrm{GV}) = pc/Ze$) is appropriate whenever the gyroradius ($r_L = R/B$) is the relevant consideration, as for acceleration via moving magnetic fields or for propagation through the magnetic fields. From column (2), for example, it follows that at a given location, for every 1000 protons that get through the geomagnetic field to reach a detector at the top of the atmosphere, there will be 157 alpha-particles, 13 nuclei with $6 \leqslant Z \leqslant 8$ and one with $21 \leqslant Z \leqslant 28$.

The number of nucleons per GeV per nucleon (column (3)) is the relevant quantity in calculating uncorrelated, secondary fluxes of particles such as pions, muons, neutrinos, antiprotons, etc. because these are essentially produced in nucleon–nucleon encounters, even when the nucleons are bound in nuclei. Though there are some specifically nuclear effects, they are small in this context. By adding up all contributions in column (3), we find that the total flux of nucleons is 23 $\mathrm{m^{-1}s^{-1}sr^{-1}GeV^{-1}}$ at 11.5 GeV/nucleon. With an integral spectral index $\gamma = 1.7$ this corresponds to the following spectrum of nucleons:

$$\frac{dN}{dE_N} = 1.7 \times 10^4 \, (E_N/\mathrm{GeV})^{-2.7} \, \frac{\text{nucleons}}{\mathrm{m^2 s\,sr\,GeV}} \quad \text{(differential)},$$
$$I(>E_N) = 10^4 (E_N/\mathrm{GeV})^{-1.7} \, \frac{\text{nucleons}}{\mathrm{m^2 s\,sr}} \quad \text{(integral)}. \tag{1.2}$$

Here E_N is total energy per nucleon and both differential and integral spectrum are given. This numerical form gives a reasonable approximation to measurements below 1000 TeV, as discussed in Chapter 2. Of the total flux in Eq. 1.2, 76.5% are free protons, 11.7% protons in nuclei and 11.8% neutrons in nuclei. The ratio $\delta_0 = (p_0 - n_0)/(p_0 + n_0) \approx 0.8$ is the fractional proton excess in the primary cosmic ray beam. The numerator is the total number of protons (including hydrogen and protons bound in nuclei) minus the number of neutrons in nuclei. The denominator is the total number of nucleons. This ratio is important for determining particle/antiparticle ratios of secondaries in the atmosphere.

Finally, total energy per nucleus is relevant for air showers because they reflect the total energy of the incident particle. The numbers in column (4) are based on measurements at 10–100 GeV/nucleon, and they only make sense for total energies in the TeV range and above where all nuclei are in the power-law regime. Adding up the contributions of all nuclei in column (4) leads to an estimate of 0.3 particles

per square meter per steradian per hour with energy greater than 100 TeV. The low rate explains why large ground-based air shower detectors are needed to explore the energy range above 100 TeV. At high energies, where the fluxes are low, it is customary to classify the primary cosmic ray nuclei above helium in groups: L (light for $3 \leqslant Z \leqslant 5$), M (medium, $6 \leqslant Z \leqslant 9$), H (heavy, $10 \leqslant Z \leqslant 20$) and VH (very heavy, $21 \leqslant Z \leqslant 30$) are standard nomenclature. The ratios are p:α:M:H:VH = 1:0.048:0.0041:0.0014:0.0003 when classified by energy/nucleon (column (1)), but 1:0.51:0.37:0.32:0.28 when classified by energy per nucleus. (We omit light nuclei here because of their low abundance, which decreases as energy increases.) Note that, when the cosmic rays are classified by total energy per nucleus, fewer than half are protons!

1.6 Energy density of cosmic rays

The mechanism for cosmic ray confinement is coupling between the charged particles and the tangled magnetic field lines that thread the interstellar medium. You can see that this is plausible by comparing the energy density of cosmic rays to the energy in magnetic fields. The relation between the energy spectrum and energy

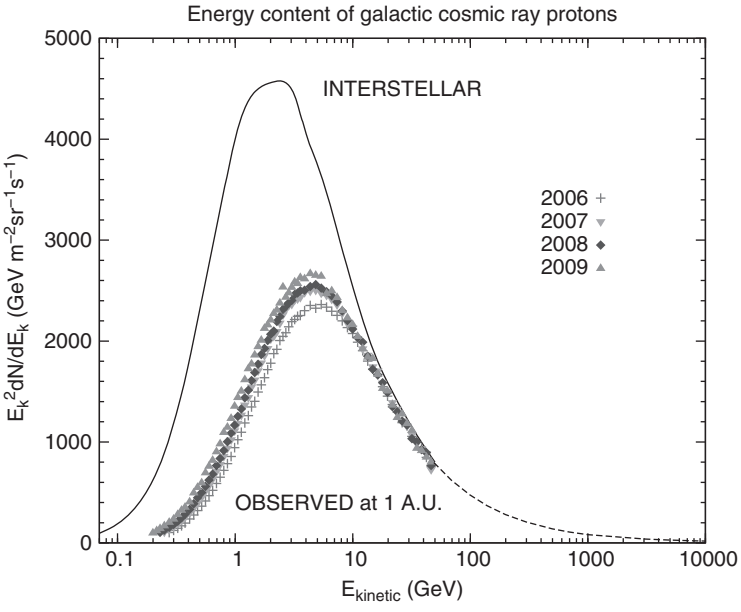

Figure 1.5 The energy flux of protons (integrand of Eq. 1.4). The data sets show measurements by the PAMELA spacecraft near Earth at various stages of the solar cycle, while the line shows an estimate of the energy flux of protons in interstellar space after correcting the data for the effect of solar modulation [4].